

 **Very Important Publication**

High-Level Production of Phenylacetaldehyde using Fusion-Tagged Styrene Oxide Isomerase

 Joel P. S. Choo,^a Richard A. Kammerer,^b Xiaodan Li,^{b,*} and Zhi Li^{a,*}
^a Department of Chemical and Biomolecular Engineering
National University of Singapore
4 Engineering Drive 4, 117585 Singapore
+65-65168416

E-mail: chelz@nus.edu.sg

^b Laboratory of Biomolecular Research, Division of Biology and Chemistry
Paul Scherrer Institut
CH-5232 Villigen PSI, Switzerland
+41-563104469
E-mail: xiao.li@psi.ch

 Manuscript received: December 2, 2020; Revised manuscript received: January 5, 2021;
Version of record online: Februar 5, 2021

 Supporting information for this article is available on the WWW under <https://doi.org/10.1002/adsc.202001500>

Abstract: An order-of-magnitude improvement in the production of phenylacetaldehyde to 3.37 M (405 g L⁻¹) from the enzymatic isomerisation of styrene oxide was achieved. A small ubiquitin-related modifier (SUMO) tag increases the productivity of the whole-cell biocatalytic system by enhancing the expression of active membrane-bound styrene oxide isomerase (SOI) while retaining enzyme catalytic efficiency and broad natural substrate scope. The isomerisation was performed by using *Escherichia coli* expressing SUMO-tagged SOI in an organic-aqueous biphasic system to yield 96% of phenylacetaldehyde.

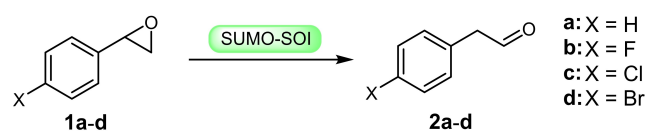
Keywords: Styrene oxide isomerase; phenylacetaldehyde; fusion enzyme; green chemistry; biotransformations; whole-cell catalysis

Introduction

Phenylacetaldehyde is a fragrance compound used in the perfume industry to give hyacinth or rose-like flavours,^[1] and can be applied in polymer manufacturing as a rate-controlling additive during ring-opening polymerisation of polyesters.^[2] It may also be used as a building block in the synthesis of pharmaceutical compounds, pesticides and other fragrance compounds such as 2-phenylethanol.^[3] As it does not occur naturally in high concentrations, industrial production of phenylacetaldehyde is typically carried out through synthetic means,^[1a] among which an important atom-efficient industrial route is the isomerisation of styrene oxide **1a** to phenylacetaldehyde **2a** catalysed by metal oxides.^[1b] Also referred to as the Meinwald rearrangement, this reaction typically involves Lewis acids,^[4] requiring toxic organic solvents such as THF,^[4d-f] as well as elevated reaction temperatures up to 200 °C.^[4a-c] Such harsh conditions lead to by-product

formation,^[4a,b] introducing difficulties in product isolation. In contrast, the biocatalytic isomerisation (Scheme 1) by styrene oxide isomerase (SOI, EC 5.3.99.7) enables an alternative route using significantly milder conditions, while achieving high selectivity with no by-product formation.^[5]

As first reported in 1989, SOI is a vital component of the epoxidation-isomerisation-oxidation metabolic pathway in styrene-degrading bacteria, found between styrene monooxygenase (SMO) and phenylacetaldehyde dehydrogenase (PAD).^[6] Isomerisation by SOI



Scheme 1. Isomerisation of styrene oxide and substituted styrene oxides by SUMO-SOI.

from *Pseudomonas sp.* VLB120^[6c] was used effectively in several publications as an intermediate step for biocatalytic cascade reactions.^[3d,e,7] However, the synthetic potential of the single-step SOI reaction to produce phenylacetaldehyde has not yet been clearly demonstrated, despite its exceptionally high activity for styrene oxide.^[6c,7] Thus far, enzymatic isomerisation of styrene oxide has been limited to the use of SOI in cell-free systems, in crude,^[5b] enriched,^[5c,d] or immobilised^[5e] forms. The highest phenylacetaldehyde concentration (322 mM, or 39 g L⁻¹) was achieved by using crude cell lysate of recombinant *E. coli* expressing SOI from *Sphingopyxis*.^[5b] Irreversible inhibition of SOI by phenylacetaldehyde had been proposed as a possible limiting factor.^[5c,e]

We therefore aimed at combining several approaches to improve the productivity of biocatalytic isomerisation by SOI. Firstly, by applying the cheaper and potentially more stable whole cells as the biocatalyst, it could be possible to achieve a high initial activity to outcompete product inhibition and attain higher product concentrations. Additionally, we sought to investigate the use of a fusion tag^[8] to improve the expression as well as stability of the enzyme in the whole-cell biocatalyst for further improvement of productivity. Moreover, biphasic aqueous-organic systems could also enhance productivity through the *in situ* removal of inhibitory aldehyde.^[5e]

We selected the SUMO (small ubiquitin-related modifier) tag as the fusion partner in the engineering of a fusion SOI enzyme, as it has been utilised effectively to improve the expression levels of the attached protein,^[9] notably membrane proteins.^[9c] In the context of biocatalysis, there is currently only one study documenting the use of the SUMO fusion tag, which was for improved operational stability at 50 °C, observed in the soluble enzyme D-psicose 3-epimerase.^[10] Therefore, the synthetic utility of the SUMO tag for whole-cell-based catalysis with a membrane-bound enzyme is as yet unknown.

In this study, we report the engineering and application of SUMO-SOI as a novel catalyst to produce **2a–d** (Scheme 1) in high concentrations, notably phenylacetaldehyde **2a** at 3.37 M (405 g L⁻¹).

Results and Discussion

The SUMO-SOI insert was prepared by splicing together the DNA sequences encoding the individual proteins by PCR, and it was subsequently cloned into pRSFduet-1 (see SI). Another pRSFduet-1 plasmid containing SOI described in a previous publication^[7a] was used as a control. Both plasmids were then transformed into *E. coli* for expression. To compare differences in active expression of the target enzyme during cell growth, *E. coli* (SUMO-SOI) and *E. coli*

(SOI) were cultured in M9 medium under the same conditions. Cell density and whole-cell specific activity for the isomerisation of styrene oxide was monitored, as shown in Figure 1A. Both cultures exhibited similar growth kinetics following induction, reaching a cell density of 4 g_{cdw} L⁻¹. Notably, the specific isomer-

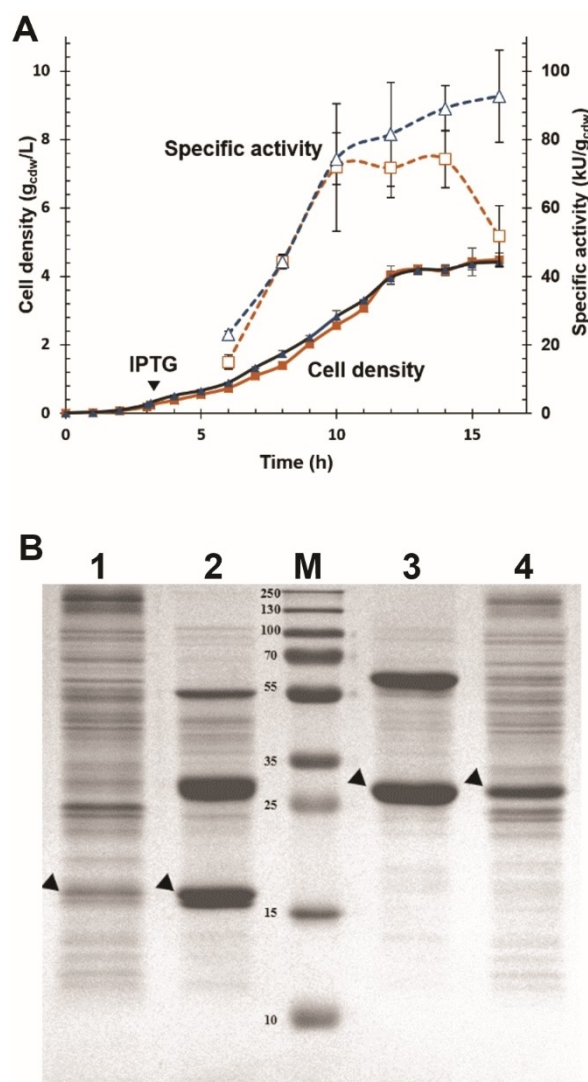


Figure 1. (A) Time-course of cell density (solid line) and specific activity (dashed line) for cell cultures of *E. coli* (SOI, ■, in orange) and *E. coli* (SUMO-SOI, ▲, in blue). The data shown represent the averages of independent cell-growth experiments performed in triplicate, with error bars indicating standard deviation. For more details, see SI. (B) SDS-PAGE for the analysis of enzyme expression in the membrane fraction of *E. coli* (SOI) and *E. coli* (SUMO-SOI). 1: Membrane proteins of *E. coli* (SOI) after DDM treatment; 2: Purified SOI; M: Protein marker. Numbers indicate molecular mass in kDa; 3: Purified SUMO-SOI; 4: Membrane proteins of *E. coli* (SUMO-SOI) after DDM treatment. Arrows indicate bands corresponding to monomeric SOI (calculated Mw: 19.7 kDa) and monomeric SUMO-SOI (calculated Mw: 30.9 kDa).

isation activity of *E. coli* (SUMO-SOI) remained higher than *E. coli* (SOI) after 10 hours, continuously increasing and reaching an impressive $93 \text{ kU g}_{\text{cdw}}^{-1}$ at 16 hours (stationary phase). In contrast, a sharp decline in the specific activity of *E. coli* (SOI) from 74 to $52 \text{ kU g}_{\text{cdw}}^{-1}$ could be observed between 14–16 hours.

To investigate whether the better whole-cell activity of *E. coli* (SUMO-SOI) was due to improved kinetics or enhanced active expression, both enzymes were purified for further characterisation. Since SOI has been reported to be an integral membrane protein,^[5c] we first isolated the membrane fractions of the cell lysates via ultracentrifugation and performed detergent solubilisation using n-dodecyl β -D-maltoside (DDM). The enzymes (both engineered with an N-terminal 6xHis tag) were then purified by Ni-NTA affinity chromatography. The SDS-PAGE gel shown in Figure 1B shows evidence of the monomeric forms of SOI (calculated Mw: 19.7 kDa) and SUMO-SOI (calculated Mw: 30.9 kDa) present in the membrane fraction (Lanes 1 and 4). After purification, a secondary band was seen for both enzymes (Lanes 2 and 3), along with a weak third band observed for SOI—a possible indication of SDS-resistant oligomeric states of both SOI and SUMO-SOI. The additional bands at 30 kDa and 55 kDa in Lane 2 most likely correspond to the dimeric and tetrameric forms of SOI respectively, while the additional band at 60 kDa in Lane 3 most likely corresponds to the dimeric form of SUMO-SOI. Based on band intensities in Lanes 1 and 4, the SUMO-SOI construct can be seen to be more highly expressed by *E. coli* following induction.

Next, we compared the specific activities for isomerisation of styrene oxide **1a**. We note that the well-established aldehyde-specific assays described in the literature^[11] are incompatible with the SOI reaction, when performed simultaneously at pH 8. Thus, a novel assay by using a second enzyme was developed, utilising the enzyme *E. coli* phenylacetaldehyde dehydrogenase (EcALDH), which readily oxidises phenylacetaldehyde with concomitant production of NADH.^[12] Product generation by SOI could therefore be coupled to NADH absorbance increase due to the

1:1 stoichiometric conversion of phenylacetaldehyde **2a** catalysed *in situ* by EcALDH. Comparing the isomerisation activities of the purified enzymes (Table 1), we found that molar activities of SOI (10.5 U nmol^{-1}) and SUMO-SOI (10.7 U nmol^{-1}) were similar, with the fusion tag retaining the catalytic efficiency of isomerisation (k_{cat}/K_m was found to be $4.09 \times 10^6 \text{ (M}\cdot\text{s)}^{-1}$ and $4.58 \times 10^6 \text{ (M}\cdot\text{s)}^{-1}$ for SUMO-SOI and SOI respectively). This provides further evidence for higher expression levels of functional SUMO-SOI (as opposed to improved kinetics) as the main reason to explain the higher whole-cell specific activities (Figure 1A) observed in *E. coli* (SUMO-SOI) compared to *E. coli* (SOI).

To explore the synthetic potential of isomerisation by SOI, we applied an aqueous-organic biphasic system: the aqueous phase contains *E. coli* resting cells suspended in potassium phosphate buffer, while the organic layer holds most of the hydrophobic substrate and product. Initially, we tested several organic solvents for the biphasic system in small-scale reactions. Solvents such as hexadecane and cyclohexane were quickly eliminated due to the poor solubility for the substrate and product. Solvents with better solubility such as toluene and hexyl acetate could give about 4 M of the product, but they are highly toxic and costly. On the other hand, organic phases such as biodiesel, ethyl oleate, and phthalate esters have been utilised effectively in biocatalytic systems as a greener solvent and to reduce contact of cells with the highly toxic styrene oxide.^[3d,e,13]

The biocatalytic isomerisation in 1:1 v/v biphasic systems was screened using the non-toxic organic solvents biodiesel, ethyl oleate and dioctyl terephthalate. Surprisingly, we observed that resting *E. coli* expressing SOI or SUMO-SOI were able to perform the isomerisation at appreciable rates even with a high styrene oxide concentration of 4 M in the organic phase (Figure 2). *E. coli* (SUMO-SOI) performed significantly better than the control *E. coli* (SOI), enhancing yields by an average of 790 mM (Figure 2A). Evidently, this was the result of the higher whole-cell activity of *E. coli* (SUMO-SOI) achieving

Table 1. Activity and kinetic data of SOI and SUMO-SOI for the isomerisation of styrene oxide.

Enzyme	Specific activity by mass of enzyme [U mg^{-1}] ^[a]	Specific activity by mole of enzyme [U nmol^{-1}] ^[b]	K_m [mM] ^[c]	k_{cat} [s^{-1}] ^[c]	k_{cat}/K_m [$\text{(M}\cdot\text{s)}^{-1}$] ^[c]
SOI	534 ± 37	10.5 ± 0.7	0.045	2.06×10^2	4.58×10^6
SUMO-SOI	345 ± 46	10.7 ± 1.4	0.049	2.01×10^2	4.09×10^6

^[a] Activity determined by using a coupled enzyme assay, by following NADH generation from EcALDH-catalysed oxidation of phenylacetaldehyde **2a** (Scheme S1) through detection of $\text{Abs}_{340\text{nm}}$ at regular time intervals. Reaction was conducted at 25 °C in a cuvette with 1 mL potassium phosphate buffer (0.05 M, pH 8) with 0.25 mM styrene oxide, 2 mM NAD^+ , 6 U of purified EcALDH and 0.15 μg of SOI or 0.27 μg of SUMO-SOI. One U is defined as 1 μmol of product formation per minute.

^[b] Determined using the calculated molecular weights of SOI (19.7 kDa) and SUMO-SOI (30.9 kDa).

^[c] Determined by non-linear regression of activity data for 0.015–0.2 mM styrene oxide (Figure S1).

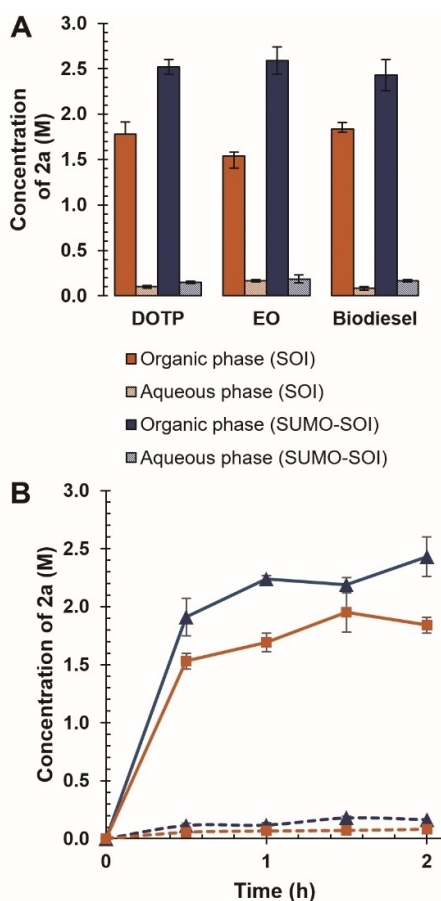


Figure 2. (A) Effect of organic phase (DOTP: dioctyl terephthalate, EO: ethyl oleate and biodiesel) on the isomerisation of 4 M styrene oxide **1a** to phenylacetaldehyde **2a** in a biphasic system of total volume 6 mL (DOTP and EO) or 30 mL (biodiesel) conducted at 30 °C for 2 hours using a 1:1 v/v mixture of organic solvent and potassium phosphate buffer (0.4 M, pH 8) containing 5 g_{cdw}L⁻¹ resting *E. coli* (SOI) or *E. coli* (SUMO-SOI) whole cells. (B) Time course of phenylacetaldehyde **2a** produced in the organic phase (solid line) and aqueous phase (dashed line) for the 30 mL biphasic biotransformation of 4 M styrene oxide **1a** conducted at 30 °C using a 1:1 v/v mixture of biodiesel and potassium phosphate buffer (0.4 M, pH 8) containing 5 g_{cdw}L⁻¹ resting *E. coli* (SOI, ■, in orange) or *E. coli* (SUMO-SOI, ▲, in blue) whole cells. All data points shown represent the averages of triplicate measurements, with error bars indicating standard deviation.

20–30% higher product yields within the first half-hour of the reaction (Figure 2B). Additionally, *in situ* removal of inhibitory aldehyde was observed in all experiments, as approximately 90–95% of the detectable product could be extracted to the organic phase in our biphasic system (Figure 2).

Encouraged by the high productivity of the system, we further performed optimisation of yields. Increasing cell density to 15 g_{cdw}L⁻¹ could push the isomerisation reaction closer to completion (Figure S2). We also

lowered reaction temperature from 30 °C to 25 °C for better enzyme stability (Figure S3). As the screened organic solvents were all equally viable for the reaction, biodiesel was chosen since it can be inexpensively obtained from sustainable sources, which would reduce the cost and environmental burden of the process.

After optimisation, the biphasic system with *E. coli* (SUMO-SOI) could attain near-quantitative yields of phenylacetaldehyde **2a** from 3.5 M styrene oxide **1a** (Table 2). No by-products were detected in the reaction, with only unreacted styrene oxide remaining (Figures S6 and S14). Assuming full extraction of the phenylacetaldehyde to the organic phase, product concentration was determined to be 3.37 M (405 gL⁻¹), an order-of-magnitude improvement over a previous report of isomerisation by SOI.^[5b] Such elevated product concentrations are not typically seen in biocatalysis and is a demonstration of the strong synthetic potential of SOI.

To explore the substrate scope and the synthetic application of the SUMO-SOI construct, we performed the isomerisation with halogen-substituted styrene oxides **1b–d** to produce the corresponding aldehydes, which are used as intermediates for pharmaceutical compounds.^[14] The products **2b–d** were sufficiently hydrophobic to be completely extracted into the organic phase, with no detectable product in the aqueous phase (Figures S14–S16). Increase in bulkiness of the substituent resulted in a decrease in product concentration, from 94 gL⁻¹ (F-substituted **2b**) to 11 gL⁻¹ (Br-substituted **2d**), likely as a result of steric interference in the binding pocket (Table 2). Nevertheless, product concentrations remained significantly higher for cells expressing SOI with the SUMO tag than without (Table 2); we even observed the complete consumption of substrate in the reaction catalysed by *E. coli* (SUMO-SOI) (Figures S8, S10 and S12). Evidently, the SUMO fusion construct retained the broad substrate scope of SOI, an indication that the N-terminal SUMO tag does not interfere with substrate binding. It might therefore serve as a useful technique for maximisation of expression levels when applied to similar membrane enzymes. While the exact mechanism of action of the SUMO tag has not yet been determined, it has been suggested that the rapid folding of the SUMO tag at the N-terminal can function as a nucleation site to encourage better expression and folding of the fused partner enzyme.^[9a]

To demonstrate the industrial feasibility of the process, a scale-up of the reaction was performed. The biodiesel applied in this study was found to be less volatile than phenylacetaldehyde, enabling product purification through distillation of the organic phase. To reduce the likelihood of product decomposition, the distillation was carried out at a lower temperature under reduced pressure. Using whole *E. coli* cells

Table 2. Isomerisation of styrene oxide and *para*-halogen-substituted styrene oxides with *E. coli* expressing SOI or SUMO-SOI.^[a]

Substrate	Substrate concentration [mM] ^[b]	Time [h]	Catalyst	Product concentration ^[b,c]		Conversion [%]
				mM	g L ⁻¹	
1 a	3500	2	<i>E. coli</i> (SOI)	3030 ± 10 ^[d]	364 ± 1 ^[d]	86.3 ± 0.2
1 a	3500	2	<i>E. coli</i> (SUMO-SOI)	3370 ± 30 ^[d]	405 ± 4 ^[d]	96.4 ± 0.9
1 b	750	2	<i>E. coli</i> (SOI)	623 ± 12	86 ± 2	83.1 ± 1.6
1 b	750	2	<i>E. coli</i> (SUMO-SOI)	681 ± 4	94 ± 1	95.0 ± 0.8
1 c	250	4	<i>E. coli</i> (SOI)	144 ± 3	22 ± 1	61.3 ± 1.4
1 c	250	4	<i>E. coli</i> (SUMO-SOI)	183 ± 4	28 ± 1	73.1 ± 1.7
1 d	100	4	<i>E. coli</i> (SOI)	39 ± 1	7.8 ± 0.2	38.6 ± 1.0
1 d	100	4	<i>E. coli</i> (SUMO-SOI)	56 ± 1	11.1 ± 0.2	56.0 ± 1.1

^[a] Biotransformation was carried out at 25 °C in 6 mL biphasic systems consisting of 1:1 v/v mixtures of biodiesel (organic phase) and potassium phosphate buffer (0.4 M, pH 8) containing 15 g_{cdw}L⁻¹ resting *E. coli* cells (aqueous phase) expressing SOI or SUMO-SOI. The data shown represent the averages of triplicate experiments, with standard errors presented.

^[b] Concentration in organic phase (assuming full extraction).

^[c] Products in the organic phase and aqueous phases were analysed by GC and HPLC respectively. For substrates **1 b–d**, no significant amounts of product were found in the aqueous phase (Figures S15–S17).

^[d] Product concentrations of **2 a** in the aqueous phase were determined to be 0.137 M (16 g L⁻¹) and 0.315 M (38 g L⁻¹) for the reactions catalysed by *E. coli* (SOI) and *E. coli* (SUMO-SOI) respectively.

expressing SUMO-SOI, a biphasic isomerisation reaction was carried out with 3.5 M of styrene oxide, in a total reaction volume of 100 ml (21 g substrate). By subjecting the biodiesel layer to a simple short-path distillation, an isolated yield of 65% (13.7 g product) could be obtained. Since phenylacetaldehyde self-polymerises by aldol condensation and acetal formation even at room temperature,^[15] product separation by distillation likely resulted in major product losses. Better isolated yields might be obtained by carrying out the distillation at lower temperatures with a stronger vacuum or by purification using column chromatography. This highly productive and simple whole-cell system has potential for scale-up and could lay the foundations for a practical biocatalytic method to produce phenylacetaldehyde.

Conclusion

In conclusion, we have developed a system for efficient enzymatic isomerisation of styrene oxide to produce phenylacetaldehyde in high concentrations and yields using SUMO-SOI expressed in *E. coli*. The SUMO tag was shown to be effective at yielding a high expression level of functional SOI while retaining catalytic efficiency. By using resting cells expressing SUMO-SOI, a higher productivity of isomerisation was achieved compared to cells expressing SOI without the SUMO tag. Phenylacetaldehyde was produced with no detectable by-products at a concentration of 405 g L⁻¹ by far the highest reported concentration for biocatalytic production of phenylacetaldehyde. By combining the productivity of whole cells with an expression-enhancing tag, we were able to significantly enhance the synthetic ability of the SOI-catalysed

reaction to a point where it could rival traditional chemical Meinwald rearrangement systems. SUMO-SOI also retained the broad natural substrate scope of SOI, enabling the production of halogen-substituted phenylacetaldehyde compounds at up to 94 g L⁻¹. Hence, the SUMO tag might even find greater synthetic utility as a tool to improve expression levels of other membrane-bound enzymes. This reported system clearly demonstrates a viable high-yielding and greener biocatalytic alternative for the isomerisation of styrene oxide and related compounds to their respective aldehydes.

Experimental Section

Engineering of *E. coli* (SUMO-SOI) and *E. coli* (SOI)

SUMO-SOI was constructed by overlap extension PCR using Phusion polymerase. Oligonucleotide primer sets (SUMO 5' BamHI, 5'-ctcgtcgatccgATGAGCGATAGCGAAGTGAACC-3' and SUMO-SOI 3', 5'-CGCGTGTAACATGCCGCCGATCTGTTACGATG-3') and (SOI 3' XhoI, 5'-TACCA-GACTCGAGTTACTACTCG-3' and SUMO-SOI 5', 5'-CATCGGCGGCATGTTACACGCGTTTG-3') were designed to amplify cDNA fragments using a synthetic SUMO gene optimised for expression in *E. coli* and SOI (*Pseudomonas sp.* VLB120),^[7a] as templates, respectively. The following PCR conditions were used: 98 °C for 1 min (1 cycle); 98 °C for 15 sec, 50 °C for 30 sec, 72 °C for 30 sec (25 cycles), 100 μL reactions. After gel extraction from a 1% agarose gel (QIAGEN QIAquick Gel Extraction Kit) 25 μL each of the amplified DNA fragments were combined and the PCR reaction repeated using primers SUMO 5' BamHI and SOI 3' XhoI. The final PCR product was purified (QIAGEN QIAquick PCR Purification Kit) and digested with 30 units each of BamHI and XhoI

restriction enzymes (NEB) for 1 h at 37 °C (100 μ L reaction volume). After purification (QIAGEN QIAquick PCR Purification Kit), the amplified product was ligated into the BamHI/XhoI site of pRSFduet-1 using Quick Ligase (NEB) (5 μ L Quick Ligase reaction Buffer (2X), 2 μ L vector, 3 μ L PCR product, 1 μ L Quick Ligase; control: H₂O instead of PCR product). After 15 min, 5 μ L of the ligation reactions were transformed in 100 μ L of chemically competent XL-1 Blue bacterial cells. After incubation on ice for 30 min, cells were heat-shocked at 42 °C for 60 sec. After cooling on ice for 2 min, cells were plated on LB plates containing 100 μ g/mL kanamycin (Kan) and incubated overnight at 37 °C. Individual colonies were grown overnight in 4 mL LB^{Kan} medium at 37 °C and recombinant plasmids were isolated (QIAGEN QIAquick Miniprep Kit). Insert sequences were verified by DNA sequencing (GATC/Eurofins).

Culture and Expression of *E. coli* for Biotransformation

E. coli (SOI) and *E. coli* (SUMO-SOI) plasmids were transformed into *E. coli* C41(DE3) Rosetta cells. Cells were grown on LB^{Kan} at 37 °C overnight. Single colonies were inoculated into 2 mL LB^{Kan} and grown for 6–8 hours (250 rpm, 37 °C). Each inoculum was subsequently transferred into a culture flask of 50–1000 mL M9 (0.1 M pH 7.5 potassium phosphate buffer, 0.5 g NaCl, 1 g NH₄Cl, 20 g glucose, 6 g yeast extract, 0.1 mM CaCl₂, 1 mM MgSO₄, and 1 mL of a 1000x trace metals solution) containing 50 μ g/mL kanamycin. OD₆₀₀ of the cultures were measured at various time points and used to calculate cell density in cell dry weight (g_{cdw}). Once OD₆₀₀ reached a value of 0.6–0.7, IPTG was added (0.5 mM final concentration), then temperature was adjusted to 22 °C for overnight growth.

Purification of SOI and SUMO-SOI

The cell pellet of 1 L of overnight M9 culture of *E. coli* (SOI) or *E. coli* (SUMO-SOI) was resuspended in lysis buffer (50 mM sodium phosphate buffer, pH 8, 0.3 M sodium chloride) and subjected to high-pressure lysis at 550 bar by an SPX Flow APV 1000 Lab Homogeniser. The cell lysate was then centrifuged at 6000 \times g for 15 min to remove unbroken cells. The remaining supernatant was subjected to high-speed centrifugation at 32300 \times g for 1 h 45 min, and the red-brown membrane pellet was then suspended in 35 mL of binding buffer (50 mM sodium phosphate buffer, pH 8, 10 mM imidazole, 0.3 M sodium chloride). 1% DDM was added, and the solution was incubated on ice for 1 hour before being centrifuged at 32300 \times g for 2 h. The solubilized red membrane fraction was then subject to affinity chromatography with the HisTrap HP column (GE Healthcare). After loading of sample, the column was washed with wash buffer 1 (50 mM sodium phosphate buffer, pH 8, 60 mM imidazole, 0.3 M sodium chloride) and wash buffer 2 (50 mM sodium phosphate buffer, pH 8, 100 mM imidazole, 0.3 M sodium chloride). Following this step, the column had a brownish-red appearance. Elution was then carried out with elution buffer (50 mM sodium phosphate buffer, pH 8, 500 mM imidazole, 0.3 M sodium chloride) until the red fraction of SOI was eluted.^[5c,16] The eluate containing purified SOI was then subject to concentration using a 30 kDa concentrator and desalted using a HiTrap

Desalting column, with desalting buffer (50 mM potassium phosphate buffer, pH 8, 0.05% DDM). SDS-PAGE was performed for the membrane fraction and purified enzymes using a 12% gel with 4–5 μ g of total protein per lane.

Measurement of Kinetic Parameters of SOI and SUMO-SOI

For isomerisation activity measurement, the following coupled enzyme assay was carried out (Scheme S1). To a 1.5 mL cuvette, 1 mL reaction for 0.25 mM ($\sim 5 K_m$) styrene oxide was carried out at 25 °C in reaction buffer (0.05 M potassium phosphate buffer, pH 8) containing 2 mM NAD⁺, 6 U EcALDH^[7b] and 0.15 μ g SOI or 0.27 μ g SUMO-SOI. Increase in absorbance at 340 nm was recorded at regular time intervals using a Hitachi U2900 spectrophotometer, and absorbance units were converted to concentration using the ϵ_{340nm} of NADH (6.22 Abs/mM/cm). The slope of the concentration-time plot for the first 15 seconds was subsequently used to determine activity, with one U defined as corresponding to one micromole of product generated in one minute. Calculated molecular weights (19659.9 Da for SOI; 30903.56 Da for SUMO-SOI) were used to determine the molar activity of the respective isomerases.

To determine kinetic parameters K_m and k_{cat} , isomerisation activity was determined with varying styrene oxide concentrations of 0.015–0.2 mM. The slope of the concentration-time plot for the first 15 seconds was used to determine the initial rate of each reaction in mM/min, to obtain a relationship between initial activity and concentration. Non-linear regression was then used to determine K_m and V_{max} based on the Michaelis-Menten model, with the MATLAB function nlinfit (Figure S1). The V_{max} calculated was further converted to k_{cat} by the relationship $k_{cat} = V_{max}/[E]$.

Isomerisation of 1 a–d to 2 a–d using *E. coli* (SOI) and *E. coli* (SUMO-SOI)

M9 cultures of the respective *E. coli* clones were centrifuged at 6000 \times g, 6 min and the pellet was washed twice, once with deionised water and once in reaction buffer (0.4 M potassium phosphate buffer, pH 8). Cell density of the resulting suspension was adjusted by repeated dilution and measuring Abs at 600 nm. In all biphasic systems described, the organic phase containing dissolved substrate 1 a–d in a known concentration was added into a conical flask containing the cell suspension. Each reaction was carried out in an orbital shaker with temperature control and shaking speed set to 250 rpm. At specific time points, 150 μ L samples of the emulsion was taken, and centrifuged at 20,000 \times g, 5 min. 10 μ L of the organic phase was subjected to GC analysis following dilution in 90 μ L ethyl acetate containing 17.32 g/L of ethylbenzene as internal standard, before being subject to further dilution in ethyl acetate (10–100 \times) for GC analysis. 12 μ L of the aqueous phase was diluted in 480 μ L acetonitrile containing 0.5 mM of benzyl alcohol as internal standard, along with 708 μ L of a quenching solution containing 0.76 M H₃PO₄ to hydrolyse unreacted styrene oxide to 1-phenyl-1,2-ethanediol (detectable by reverse phase HPLC, see Figure S13). The sample was then filtered through a 0.2 μ L Minisart RC4 filter into a vial for reverse phase HPLC analysis.

Preparative Biotransformation of Styrene Oxide **1a** to Produce Phenylacetaldehyde **2a**

To 50 mL of resting *E. coli* (SUMO-SOI) cell suspension (0.4 M potassium phosphate buffer, pH 8) of cell density $15 \text{ g}_{\text{cdw}}/\text{L}$ in a 500 mL conical flask, 50 mL of biodiesel containing 3.5 M of styrene oxide **1a** (21.03 g) was added. The reaction was carried out for 2 h at 25 °C in an orbital shaker set at 250 rpm. 5 mL of H_3PO_4 (85 wt%) was then added to quench the reaction, followed by 10 minutes of incubation to completely hydrolyse any remaining styrene oxide. The reaction mixture was then saturated with NaCl and transferred to two centrifuge tubes for centrifugation at $15000 \times g$ for 10 min. The organic phase was then carefully transferred to a 50 mL round-bottomed flask and distilled under reduced pressure in two batches, using the short-path distillation setup shown in Figure S4. Distillation temperature: 100–140 °C. Isolated yield: 13.66 g. Appearance: clear liquid.

Phenylacetaldehyde **2a**: ^1H NMR (400 MHz, CDCl_3) δ 9.78–9.73 (t, 1H, $J=2.4$ Hz, CHO), 7.41–7.35 (m, 2H, ArH), 7.34–7.28 (m, 1H, ArH), 7.25–7.20 (m, 2H, ArH), 3.69 (d, $J=2.4$ Hz, 2H, CH_2). ^{13}C NMR (400 MHz, CDCl_3) δ 199.59, 131.97, 129.75, 129.15, 127.56, 50.72. HRMS (APCI-): m/z 119.0501 (Calcd. for $[\text{M}-\text{H}]^-$: 119.0502)

Preparative Biotransformation of Substituted Styrene Oxide **1b–d** to Produce the Corresponding Phenylacetaldehydes **2b–d**

To 30 mL of resting *E. coli* (SUMO-SOI) cell suspension (0.4 M potassium phosphate buffer, pH 8) of cell density $15 \text{ g}_{\text{cdw}}/\text{L}$ in a 125 mL conical flask, 15 mL of DOTP containing 0.75 M or 0.25 M of **1b** or **1c** was added respectively; to 50 mL of resting *E. coli* (SUMO-SOI) cell suspension (0.4 M potassium phosphate buffer, pH 8) of cell density $15 \text{ g}_{\text{cdw}}/\text{L}$ in a 500 mL conical flask, 30 mL of biodiesel containing 0.25 M of **1d** was added. The reactions were carried out for 2 h in an orbital shaker set at 250 rpm. The reaction mixtures were then saturated with NaCl and placed into a centrifuge tube for centrifugation at $15000 \times g$ for 10 min. The organic phases were then carefully transferred to a 50 mL round-bottomed flask and distilled under reduced pressure to obtain a crude distillate. Distillation temperatures: 100–135 °C (**2b**); 130–160 °C (**2c**); 150–180 °C (**2d**). As the products were found to be insufficiently pure, a further purification was performed using a short silica column (1:20 ethyl acetate:hexane) and the fractions with highest purity were dried with sodium sulfate and used as product standards.

(4-Fluorophenyl)acetaldehyde **2b**: ^1H NMR (400 MHz, CDCl_3) δ 9.74 (t, $J=2.2$ Hz, 1H, CHO), 7.21–7.14 (m, 2H, ArH), 7.10–7.01 (m, 2H, ArH), 3.68 (d, $J=2.2$ Hz, 2H, CH_2). ^{13}C NMR (400 MHz, CDCl_3) δ 198.98, 162.23 (d, $J=246.1$ Hz), 131.18 (d, $J=8.1$ Hz), 127.54 (d, $J=3.3$ Hz), 115.91 (d, $J=21.4$ Hz), 49.66. HRMS (APCI-): m/z 137.0412 (Calcd. for $[\text{M}-\text{H}]^-$: 137.0408)

(4-Chlorophenyl)acetaldehyde **2c**: ^1H NMR (400 MHz, CDCl_3) δ 9.75 (t, $J=2.1$ Hz, 1H, CHO), 7.39–7.27 (m, 2H, ArH), 7.19–7.11 (m, 2H, ArH), 3.68 (d, $J=2.2$ Hz, 2H, CH_2). ^{13}C NMR (400 MHz, CDCl_3) δ 198.64, 133.51, 130.95, 130.27, 129.15,

49.81. HRMS (APCI-): m/z 153.0114 (Calcd. for $[\text{M}-\text{H}]^-$: 153.0113)

(4-Bromophenyl)acetaldehyde **2d**: ^1H NMR (400 MHz, CDCl_3) δ 9.74 (t, $J=2.1$ Hz, 1H, CHO), 7.54–7.44 (m, 2H, ArH), 7.13–7.05 (m, 2H, ArH), 3.67 (d, $J=2.1$ Hz, 2H, CH_2). ^{13}C NMR (400 MHz, CDCl_3) δ 198.51, 132.11, 131.30, 130.78, 121.57, 49.87. HRMS (APCI-): m/z 196.9603 (Calcd. for $[\text{M}-\text{H}]^-$: 196.9608)

Acknowledgements

We acknowledge financial support for this work from the Ministry of Education, Singapore through an MOE Tier 2 Grant (MOE 2016-T2-2-140; NUS WBS R-279-000-501-112).

References

- [1] a) C. Kohlpaintner, M. Schulte, J. Falbe, P. Lappe, J. Weber, in *Ullmann's Encyclopedia of Industrial Chemistry*, Wiley-VCH Verlag GmbH & Co. KGaA, Weinheim, Germany, **2000**, pp. 1–39; b) C. Kohlpaintner, M. Schulte, J. Falbe, P. Lappe, J. Weber, G. D. Frey, in *Ullmann's Encyclopedia of Industrial Chemistry*, Wiley-VCH Verlag GmbH & Co. KGaA, Weinheim, Germany, **2013**, pp. 1–7; c) J. Panten, H. Surburg, in *Ullmann's Encyclopedia of Industrial Chemistry*, Wiley-VCH Verlag GmbH & Co. KGaA, Weinheim, Germany, **2016**, pp. 1–45.
- [2] E. Hosseini Nejad, A. Paoniasari, C. E. Koning, R. Duchateau, *Polym. Chem.* **2012**, *3*, 1308–1313.
- [3] a) X. Zhang, S. Sarkar, R. C. Larock, *J. Org. Chem.* **2006**, *71*, 236–243; b) P. B. Rasmussen, S. Bøwadt, *Synthesis* **1989**, *1989*, 114–117; c) M. Sakai, H. Hirata, H. Sayama, K. Sekiguchi, H. Itano, T. Asai, H. Dohra, M. Hara, N. Watanabe, *Biosci. Biotechnol. Biochem.* **2007**, *71*, 2408–2419; d) B. R. Lukito, S. Wu, H. J. J. Saw, Z. Li, *ChemCatChem* **2019**, *11*, 831–840; e) B. S. Sekar, B. R. Lukito, Z. Li, *ACS Sustainable Chem. Eng.* **2019**, *7*, 12231–12239.
- [4] a) R. Umeda, M. Muraki, Y. Nakamura, T. Tanaka, K. Kamiguchi, Y. Nishiyama, *Tetrahedron Lett.* **2017**, *58*, 2393–2395; b) X.-F. Zhang, J. Yao, X. Yang, *Catal. Lett.* **2017**, *147*, 1523–1532; c) R. Srirambalaji, S. Hong, R. Natarajan, M. Yoon, R. Hota, Y. Kim, Y. Ho Ko, K. Kim, *Chem. Commun. (Camb.)* **2012**, *48*, 11650–11652; d) N. Humbert, D. J. Vyas, C. Besnard, C. Mazet, *Chem. Commun. (Camb.)* **2014**, *50*, 10592–10595; e) D. J. Vyas, E. Larionov, C. Besnard, L. Guenee, C. Mazet, *J. Am. Chem. Soc.* **2013**, *135*, 6177–6183; f) I. Karamé, M. L. Tommasino, M. Lemaire, *Tetrahedron Lett.* **2003**, *44*, 7687–7689; g) M. W. C. Robinson, K. S. Pillinger, I. Mabbett, D. A. Timms, A. E. Graham, *Tetrahedron* **2010**, *66*, 8377–8382.
- [5] a) R. Kourist, P. Domínguez de María, K. Miyamoto, *Green Chem.* **2011**, *13*, 2607–2618; b) M. Oelschlagel, L. Richter, A. Stühr, S. Hofmann, M. Schlomann, *J. Biotechnol.* **2017**, *252*, 43–49; c) M. Oelschlagel, J. A.

- Groning, D. Tischler, S. R. Kaschabek, M. Schlomann, *Appl. Environ. Microbiol.* **2012**, *78*, 4330–4337; d) M. Oelschlagel, J. Zimmerling, M. Schlomann, D. Tischler, *Microbiology (Reading)* **2014**, *160*, 2481–2491; e) M. Oelschlagel, A. Riedel, A. Zniszczol, K. Szymanska, A. B. Jarzebski, M. Schlomann, D. Tischler, *J. Biotechnol.* **2014**, *174*, 7–13.
- [6] a) S. Hartmans, J. P. Smits, M. J. Van der Werf, F. Volkering, J. A. M. De Bont, *Appl. Environ. Microbiol.* **1989**, *55*, 2850–2855; b) M. Oelschlagel, J. Zimmerling, D. Tischler, *Front. Microbiol.* **2018**, *9*, 1–17; c) S. Panke, B. Witholt, A. Schmid, M. G. Wubbolts, *Appl. Environ. Microbiol.* **1998**, *64*, 2032–2043.
- [7] a) S. Wu, J. Liu, Z. Li, *ACS Catal.* **2017**, *7*, 5225–5233; b) S. Wu, Y. Zhou, D. Seet, Z. Li, *Adv. Synth. Catal.* **2017**, *359*, 2132–2141.
- [8] H. Yang, L. Liu, F. Xu, *Appl. Microbiol. Biotechnol.* **2016**, *100*, 8273–8281.
- [9] a) J. G. Marblestone, S. C. Edavettal, Y. Lim, P. Lim, X. Zuo, T. R. Butt, *Protein Sci.* **2006**, *15*, 182–189; b) M. P. Malakhov, M. R. Mattern, O. A. Malakhova, M. Drinker, S. D. Weeks, T. R. Butt, *J. Struct. Funct. Genomics* **2004**, *5*, 75–86; c) X. Zuo, S. Li, J. Hall, M. R. Mattern, H. Tran, J. Shoo, R. Tan, S. R. Weiss, T. R. Butt, *J. Struct. Funct. Genomics* **2005**, *6*, 103–111.
- [10] S. N. Patel, M. Sharma, K. Lata, U. Singh, V. Kumar, R. S. Sangwan, S. P. Singh, *Bioresour. Technol.* **2016**, *216*, 121–127.
- [11] a) R. Lauchli, K. S. Rabe, K. Z. Kalbarczyk, A. Tata, T. Heel, R. Z. Kitto, F. H. Arnold, *Angew. Chem. Int. Ed. Engl.* **2013**, *52*, 5571–5574; b) C. S. Mesquita, R. Oliveira, F. Bento, D. Geraldo, J. V. Rodrigues, J. C. Marcos, *Anal. Biochem.* **2014**, *458*, 69–71; c) M. Horvat, T. S. Larch, F. Rudroff, M. Winkler, *Adv. Synth. Catal.* **2020**, *362*, 4673–4679.
- [12] J. S. Rodriguez-Zavala, A. Allali-Hassani, H. Weiner, *Protein Sci.* **2006**, *15*, 1387–1396.
- [13] a) H. Toda, R. Imae, N. Itoh, *Tetrahedron: Asymmetry* **2012**, *23*, 1542–1549; b) D. Kuhn, M. K. Julsing, E. Heinzle, B. Bühler, *Green Chem.* **2012**, *14*, 645–653; c) J. H. Han, M. S. Park, J. W. Bae, E. Y. Lee, Y. J. Yoon, S.-G. Lee, S. Park, *Enzyme Microb. Technol.* **2006**, *39*, 1264–1269.
- [14] a) J. U. Peters, H. Kuhne, H. Dehmlow, U. Grether, A. Conte, D. Hainzl, C. Hertel, N. A. Kratochwil, M. Otteneder, R. Narquizian, C. G. Panousis, F. Ricklin, S. Rover, *Bioorg. Med. Chem. Lett.* **2010**, *20*, 5426–5430; b) Y. Haga, S. Mizutani, A. Naya, H. Kishino, H. Iwaasa, M. Ito, J. Ito, M. Moriya, N. Sato, N. Takenaga, A. Ishihara, S. Tokita, A. Kanatani, N. Ohtake, *Bioorg. Med. Chem.* **2011**, *19*, 883–893; c) M. Brindisi, S. Maramai, S. Gemma, S. Brogi, A. Grillo, L. Di Cesare Mannelli, E. Gabellieri, S. Lamponi, S. Saponara, B. Gorelli, D. Tedesco, T. Bonfiglio, C. Landry, K. M. Jung, A. Armirotti, L. Luongo, A. Ligresti, F. Piscitelli, C. Bertucci, M. P. Dehouck, G. Campiani, S. Maione, C. Ghelardini, A. Pittaluga, D. Piomelli, V. Di Marzo, S. Butini, *J. Med. Chem.* **2016**, *59*, 2612–2632; d) X. D. Wang, W. Wei, P. F. Wang, L. C. Yi, W. K. Shi, Y. X. Xie, L. Z. Wu, N. Tang, L. S. Zhu, J. Peng, C. Liu, X. H. Li, S. Tang, Z. P. Xiao, H. L. Zhu, *Bioorg. Med. Chem.* **2015**, *23*, 4860–4865.
- [15] J. L. E. Brickson, G. N. Grammer, *J. Am. Chem. Soc.* **1958**, *80*, 5466–5469.
- [16] D. Tischler, *Microbial Styrene Degradation*, 1st ed., Springer International Publishing, **2015**.